# Thermodynamic and Transport Properties of Crown-Ethers: Force Field Development and Molecular Simulations

Seyed Hossein Jamali, Mahinder Ramdin, Tim M. Becker, Shwet Kumar Rinwa, Wim Buijs, and Thijs J. H. Vlugt*

Engineering Thermodynamics, Process & Energy Department, Faculty of Mechanical, Maritime and Materials Engineering, Delft University of Technology, Leeghwaterstraat 39, 2628CB Delft, The Netherlands

S Supporting Information

ABSTRACT: Crown-ethers have recently been used to assemble porous liquids (PLs), which are liquids with permanent porosity formed by mixing bulky solvent molecules (e.g., 15-crown-5 ether) with solvent-inaccessible organic cages. PLs and crown-ethers belong to a novel class of materials, which can potentially be used for gas separation and storage, but their performance for this purpose needs to be assessed thoroughly. Here, we use molecular simulations to study the gas separation performance of crown-ethers as the solvent of porous liquids. The TraPPE force field for linear ether molecules has been adjusted by fitting a new set of torsional potentials to accurately describe cyclic crown-ether molecules. Molecular dynamics (MD) simulations have been used to compute densities, shear viscosities, and self-diffusion coefficients of 12-crown-4, 15-crown-5, and 18-crown-6 ethers. In addition, Monte Carlo (MC) simulations have been used to compute the solubility of the gases CO_2, CH_4, and N_2 in 12-crown-4 and 15-crown-5 ether. The computed properties are compared with available experimental data of crown-ethers and their linear counterparts, i.e., polyethylene glycol dimethyl ethers.
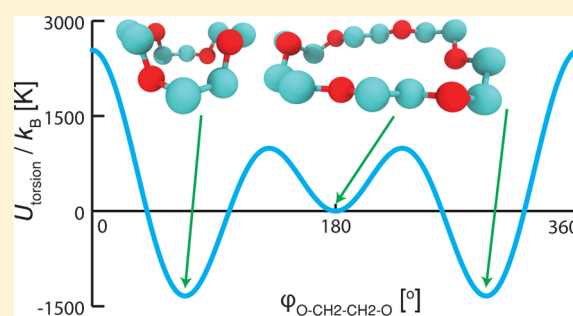
INTRODUCTION

Crown-ethers are macrocyclic polyethers discovered by Pedersen in the late 1960s.[1] Due to their strong ability to complex with cations and to solvate salts in aprotic solvents, crown-ethers have been used in phase-transfer catalysis, sensors, solvent extraction, analytical chemistry, biochemistry, and electrochemistry.[1−6] Recently, crown-ethers have been used to synthesize the first generation of porous liquids (PLs), which are liquids with permanent pores, a unique property not exhibited by conventional solvents.[7−11] Porous liquids can be created by mixing organic cage molecules with bulky solvents, such as crown-ethers, which cannot enter the pores of the cage molecules, thereby the porosity of the cages in the mixture is maintained.[7] The pores can accommodate small guest molecules, which renders PLs interesting candidates for gas separation and storage.[7,12−16] The performance of PLs in gas separation is strongly dependent on the transport and thermodynamic properties of the crown-ether solvent. In the past, some molecular simulation studies[17−25] investigated the specific application of cation complexation with crown-ethers in (organic) solvents. However, the feasibility of using crown-ethers as gas absorption solvents has not been experimentally or computationally explored so far.

In this study, molecular simulation is used to investigate the potential of crown-ethers for gas separation purposes. A schematic representation of the studied crown-ether molecules is shown in Figure 1. The ligand cavity radii of 12-crown-4, 15-crown-5, and 18-crown-6 are 0.6, 0.85, and 1.3 Å, respectively.[4]
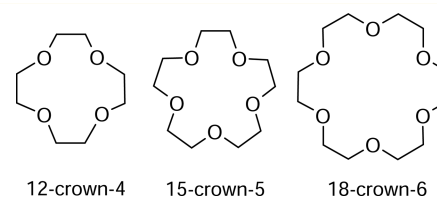
Figure 1. Schematic representation of the studied crown-ethers.

Hence, crown-ethers can complex cations of similar size selectively, e.g., 12-crown-4 has a high affinity for Li^+, which has an ionic radius of 0.74 Å.[4] We are interested in the affinity of crown-ethers for separating (neutral) gas molecules. To design a separation process, data on transport properties and gas solubilities are required. Molecular dynamics (MD) simulation is used to compute densities, viscosities, and self-diffusion coefficients of 12-crown-4, 15-crown-5, and 18-crown-6 ethers, while Monte Carlo (MC) simulations are used to compute the solubility of CO_2, CH_4, and N_2 in 12-crown-4 and 15-crown-5.

Computed properties in molecular simulations are strongly dependent on the employed force field. As mentioned earlier, several studies have studied the complexation of crown-ethers using MD simulations. Most of these studies[17,19−21,23−27]

Table 1. Dihedral Parameters of the Linear Ether TraPPE Force Field and the Refitted Torsional Potentials[a]

force field	C−C−O-C				O−C−C-O			
	c_0	c_1	c_2	c_3	c_0	c_1	c_2	c_0
linear ether TraPPE[32]	0.00	725.35	−163.75	558.20	503.24	0.00	−251.62	1006.47
refined TraPPE	136.4	1523.2	−613.4	473.0	0.0	163.0	−964.7	1106.1

[a]All force constants (c_i) are in $c_i/k_B/K$.

employed the AMBER[28] force field or its variants. In this study, we use the transferable potentials for phase equilibria (TraPPE) force field,[29] which is a united-atom force field. Contrary to the all-atom AMBER force field, the united-atom TraPPE force field lumps hydrogen atoms in with the bonded carbon atoms. This means that the AMBER force field is computationally expensive as more interaction sites are considered. Moreover, the parameters of the TraPPE force field are transferable to other hydrocarbons and these parameters are compatible with natural gas or syngas components, such as CO_2[30] and H_2S.[31] The transferability of force field parameters as well as compatibility with the force field of molecules present in the gas treatment processes are the main merits of choosing this force field. However, the TraPPE force field was developed for linear ether molecules,[32] so the force field parameters for cyclic ether molecules are adjusted here using the density functional theory (DFT) prior to be used in MD simulations. All computed properties are compared with limited experimental data and overall a good agreement is found. These simulation results show that the applied force field is able to describe the crown-ether systems, which can serve as a basis to study the more complex PLs.

■ FORCE FIELD DEVELOPMENT

The united-atom (UA) TraPPE force field[32] for ethers seems to be a good starting point for the force field-based molecular simulations of crown-ethers. The force field parameters of ether groups were originally developed for linear molecules,[32] so the parameters may not be transferable to cyclic molecules. This issue was also addressed by Keasler et al.[33] who fitted the TraPPE force field parameters of five or six-atom membered cyclic molecules. We shall adopt the same approach when defining new force field parameters for crown-ethers, or generally for any ether group in cyclic molecules. The bond stretching and bond-angle bending potentials are considered to be identical to the TraPPE-UA force field as they do not vary significantly even for small five or six-membered cyclic molecules.[33] The nonbonded potential parameters of cyclic and linear molecules may slightly vary according to the different polarization of atoms in these two types of molecules. However, it is expected that this effect will become less significant as the diameter of the ring increases and the atoms in the ring are further located from each other.[33] Therefore, we do not consider modification of the original Lennard-Jones parameters and partial atomic charges provided by the TraPPE-UA force field.[32] The only force field component requiring adjustment is the intramolecular torsional potential, specified by the alteration of the dihedral angle. A similar approach to the work of Keasler et al.[33] is used to obtain the force field parameters of the torsional potential. By scanning a wide range of variation for the torsion types present in a single molecule, the energy profile computed from the DFT is fitted to a functional form for each torsion type. The TraPPE functional

form of torsional potential for a dihedral angle ϕ consists of a cosine series with four force constants (c_0, c_1, c_2, and c_3):[32]

$$U_{torsion}(\phi) = c_0 + c_1[1 + \cos(\phi)] + c_2[1 - \cos(2\phi)] + c_3[1 + \cos(3\phi)] \tag{1}$$

The torsional potential is fitted so that the total force field-based energy, including the bonded and nonbonded interactions, reproduces the DFT energy. Initially, the most stable conformer of a molecule is identified according to DFT calculations. This configuration has the minimum energy level out of all possible conformers of that molecule or, in other words, the highest Boltzmann probability. Constraining one of the dihedral angles in the molecule to a constant value and then relaxing the structure with the help of DFT calculations leads to a new shape and a new energy level. By modifying the dihedral angle for a range of values, different energy levels of the molecule can be scanned. The energy differences from the ground-state energy level are then computed from the DFT (ΔU_{DFT}) and molecular mechanics (ΔU_{ff}). DFT calculations are carried out at the B3LYP/6-31G* level in SPARTAN 14.0.[34] The term ΔU_{ff} consists of all bonded and nonbonded energies that have been specified by the TraPPE force field except for the torsional potential. In this process, the relative energy of N_{conf} distinct configurations of the molecule is scanned. The force constants specified in eq 1 are then obtained by minimizing the absolute difference between the DFT and molecular mechanics energies ($\Delta\Delta U_i$) with the help of the following objective function:

$$O. F. = \frac{1}{N_{conf}} \sum_{i=1}^{N_{conf}} |\Delta\Delta U_i| \tag{2}$$

Crown-ethers have two torsion types: $CH_2-CH_2-O-CH_2$ and $O-CH_2-CH_2-O$ (represented as C−C−O−C and O−C−C−O), each of which requires four torsional potential parameters according to eq 1. Due to the ring structure of crown-ethers, modifying a dihedral angle also alters other degrees of freedom of the molecule, namely bond stretching, bond-angle bending, and dihedral-angle torsion. Therefore, all force field parameters should be fitted simultaneously. In total, 63 and 104 different configurations of 12-crown-4 and 18-crown-6 molecules are considered for this force field parametrization, respectively. The objective function (eq 2) is minimized via the interior point method (the fmincon function) implemented in the MATLAB Optimization Toolbox.[35] For this data set, the final value of the objective function is 110 K/k_B (0.22 kcal/mol). The fitted force constants are provided in Table 1 and the shape of the two torsion types over different dihedral angles is illustrated in Figure 2.

We initially noticed the need to refit new torsional potential when the TraPPE force field for linear ethers (linear ether TraPPE force field) could not reproduce the liquid form of 12-crown-4 at room or elevated temperatures. In contrast to experiments, MD simulations based on the linear ether TraPPE
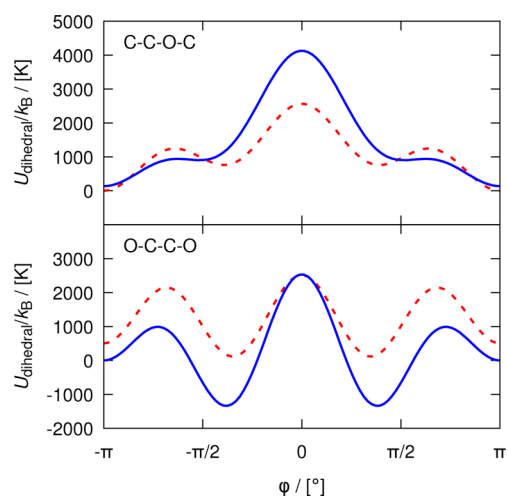
Figure 2. Fitted torsional potential (Table 1) compared to the torsional potential of the linear ether TraPPE torsional force field (red dashed lines).

Figure 3. Comparison between torsional potentials computed for all dihedral angles of the first 10 conformers of 12-crown-4 (red squares), 15-crown-5 (blue circles), and 18-crown-6 (green diamonds) optimized using the DFT calculations and the newly fitted torsional potential.

force field predict a crystal form of 12-crown-4 (see the Supporting Information). In the first place, a set of configurations of 12-crown-4 was considered for the force field parametrization. Despite the better performance of the first fitted torsional potential for 12-crown-4, the computed transport properties of 18-crown-6 deviated by 1 order of magnitude from the experiments (not reported here). The reason can be found in the difference between the shape of 12-crown-4 and 18-crown-6 molecules (shown in the Supporting Information). 12-crown-4 is a small cyclic molecule, so it has only gauche orientations for its O−C−C−O dihedral angles. The gauche orientation is visible in its prevalent conformer (with a Boltzmann probability of 90% at 298 K) whose dihedral angles are equal to either −72° or +72° at the B3LYP/6-31G* DFT level. As the size of crown increases, the cyclic molecule can have at least one trans O−C−C−O dihedral angle, which is not present in smaller crowns. Therefore, the force constants fitted to the 12-crown-4 energy profile does not contain any information on the energy of the O−C−C−O dihedral angles in the vicinity of $\phi = \pi$, which is present in the main conformer of 18-crown-6. The final force constants (Table 1) are obtained by fitting to the energy profiles of both 12-crown-4 and 18-crown-6.

To examine how accurately the new (refined TraPPE) force field can reproduce the torsional potential of DFT calculations, the torsional energies of the first ten conformers of the three crown-ethers were compared between the DFT and molecular mechanics. The cumulative Boltzmann probability of these ten conformers at 298 K for each molecule is at least 95%, encompassing a large portion of the possible crown-ether configurations. Initially, these conformers were relaxed using DFT calculations at the B3LYP/6-31G* level. The torsional energy of each dihedral angle ($U_{dihedral,DFT}$) is computed from eq 1 with the newly fitted parameters in Table 1. Each configuration was then relaxed using molecular mechanics based on the new force field. Similarly, the torsional energies of the relaxed configuration are also calculated from eq 1. Figure 3 shows the comparison of these 30 conformers and their corresponding 150 O−C−C−O and 300 C−C−O−C torsional energy data points. Most of the dihedral angles and consequently their energy levels show small deviations. About 93% of the 450 dihedral angles shows a maximum deviation in
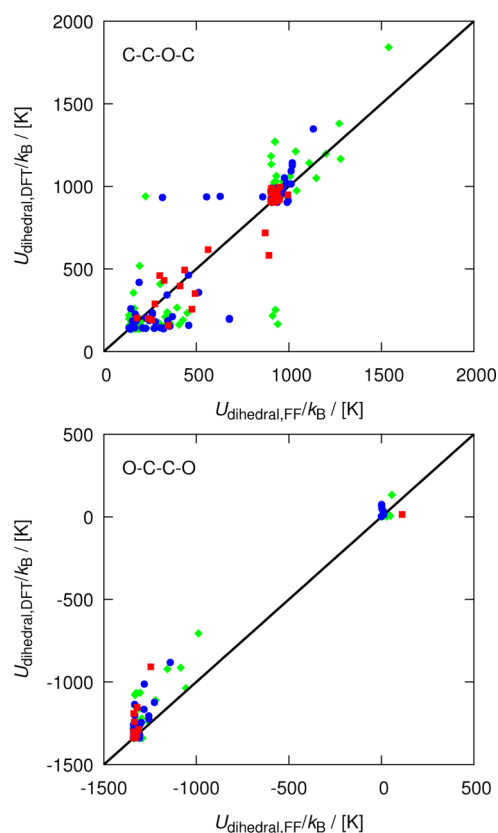
the torsional energy of 250 K/k_B (0.5 kcal/mol) from DFT calculations. It is worth mentioning that the current force field parameters were obtained by varying the dihedral angles of only one conformer of 12-crown-4 and one conformer of 18-crown-6. However, the fitted parameters may in general be used for all crown-ethers. In the next stage, the accuracy of the force field parameters has to be verified by computing thermodynamic/transport properties of crown-ethers and compare them with experimental data.

■ SIMULATION DETAILS

Force field-based Monte Carlo (MC) and molecular dynamics (MD) simulations are two powerful methods to study the thermodynamic and transport properties of materials. In this study, we use RASPA[36,37] and LAMMPS[38] for our MC and MD simulations. The force field parameters of crown-ethers,[32] CH_4,[29] CO_2,[30,39] and N_2[30] are listed in the Supporting Information. The Lennard-Jones (LJ) potentials are truncated at 12 Å and analytic tail corrections are applied for the computation of energy and pressure. The Lorentz−Berthelot combining rules are applied for dissimilar interaction sites.[40] The long-range electrostatic interactions are included by means of the Ewald summation with a relative precision of 10^{-5}.[41]

MD simulations provide the tool for studying the dynamics of molecules in fluids or, in other words, their transport properties. There are several approaches to computing transport properties such as shear viscosity[42−46] or diffusion coefficients.[47] Here, we carry out equilibrium MD (EMD)

simulations to calculate the transport properties of crown-ethers with the help of the Einstein relations, which were described in the literature.[40,48,49] The order-n algorithm is employed to sample time correlations in the EMD simulations,[50] thus resulting in better statistics than the conventional algorithm.[41] The equations of motion are integrated by the use of the velocity-Verlet algorithm with a time step size of 1 fs.[41] Accordingly, the duration of the equilibration and production stages in the NPT and NVT ensemble are 15 ns. The time correlations are sampled in the NVE ensemble with a total simulation length of 400 ns. Such a long simulation is necessary as the fluid becomes more viscous and longer time-correlations with better statistics are required.

Thermodynamic properties such as solubilities of gases in solvents are calculated using MC simulations. Computing the solubility of gases in nonvolatile solvents requires an open ensemble in which a reservoir comes into contact with the simulation box containing the solvent. This is the osmotic ensemble in which the absorption isotherms of the gases in the low-volatile crown-ethers are computed.[51] In this ensemble, the temperature, pressure, the number of solvent molecules in the liquid, and the fugacity of the solute are kept fixed.[51,52] In our previous work, we studied the solubility of natural gas, synthesis gas, or acidic gas components in commercial solvents as well as ionic liquids.[48,53−56] The results were verified on the basis of the available experimental data. Good agreement between the experiments and simulations indicates the capability of this method in predicting gas solubility data.

Four types of MC trial moves are used: translations, rotations, insertions/deletions of gas molecules, and volume changes. The probability of selecting the first two trial moves is 40% and the insertions/deletions trial move is 20%. The volume change trial move is chosen randomly every 1000 trial moves. Crown-ethers are cyclic molecules; it is therefore not possible in RASPA to use configurational-bias Monte Carlo (CBMC) trial moves to generate different configurations of the molecule. This means that all crown-ether molecules are considered to be rigid in MC simulations. The rigid configuration is obtained from the conformer with the highest Boltzmann probability based on the conducted DFT calculations. While this approach may work for small molecules, the importance of using flexible molecules becomes more pronounced as the size of the molecule increases. Therefore, we exclusively study the solubility of gases in 12-crown-4 and 15-crown-5 ethers. Each MC simulation consists of half a million equilibration MC cycles, followed by one million production MC cycles. It is one MC cycle that is equal to the number of particles in the system. The gas solubility at a given temperature and pressure is computed from 4 and 8 independent simulations of 12-crown-4 and 15-crown-5, respectively.

■ RESULTS AND DISCUSSION

The refined TraPPE force field is applied to calculate the thermodynamic and transport properties of three crown-ethers, that are 12-crown-4, 15-crown-5, and 18-crown-6. In this section, we report the properties of the pure crown-ethers and their mixtures as well as the vapor−liquid equilibrium (VLE) results of three natural gas components in 12-crown-4 and 15-crown-5.

Properties of Pure Crown-Ethers. Figure 4 shows the densities of the crown-ethers, computed for both the linear ether TraPPE and the refined TraPPE force fields and a comparison with the experimental densities. The refined
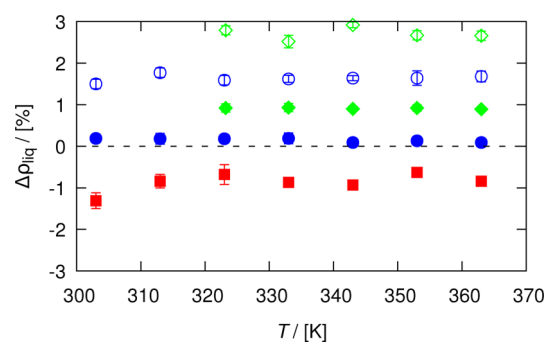

Figure 4. Relative error in calculated densities of 12-crown-4 (red), 15-crown-5 (blue), and 18-crown-6 (green) at different temperatures based on the linear ether TraPPE (open symbols) and the refined TraPPE (closed symbols) force fields. The simulation results are available in the Supporting Information.

TraPPE force field (closed symbols) provides an accurate estimate of the densities with less than 1% deviation from the experiments, for a wide range of temperatures. In comparison, the linear ether TraPPE force field estimates the experimental densities of 15-crown-5 and 18-crown-6 with deviations of 3%. Furthermore, the linear ether TraPPE force field substantially overpredicts the density of 12-crown-4 (approximately 1200 kg/m^3). We observed a crystalline arrangement and no Brownian motion of the 12-crown-4 molecules in the simulations (see the Supporting Information), which shows that such a high density corresponds to a solid state rather than a liquid state at room/elevated temperatures. This considerable discrepancy between the simulations and the experiments was the main rationale behind the development of the refined TraPPE force field for cyclic ether molecules.

Before proceeding with the analysis of the computed transport properties, it is necessary to address the effect of a finite-size system in molecular simulations on the computed transport properties. It has been observed that as the number of particles/molecules in a simulation box increases, the computed self-diffusion coefficient increases linearly by the length of the simulation box (L):[57]

$$D_\infty = D_{MD} + \frac{\xi k_B T}{6\pi\eta L} \tag{3}$$

where D_∞ and D_{MD} are the respective self-diffusion coefficients in the thermodynamic limit and finite-size system. ξ is a constant value, which is equal to 2.837297 for cubic simulation boxes.[57] k_B, T, and η are the Boltzmann constant, temperature, and viscosity of the system. Henceforth, we refer to the last term of eq 3 as the Yeh and Hummer (YH) correction.[57] Despite the evident finite-size effect on the self-diffusion coefficient, no specific system-size effect on the viscosity has been observed.[57,58] Moultos et al.[58] carried out MD simulations for different fluids, such as CO_2, long hydrocarbons, and glymes to study the applicability of the YH correction in rather complex systems. These authors recognized that correcting self-diffusion for finite-size systems is necessary and that including the YH correction provides a better estimate of the self-diffusion coefficient in the thermodynamic limit. We use a relatively small number of particles in all our simulations, so it is expected that the system-size effect is not negligible in these cases and the YH correction is indispensable. To verify how accurate the YH correction is, two additional system sizes for the pure 12-crown-4 at 363 K were studied. Figure 5 shows the
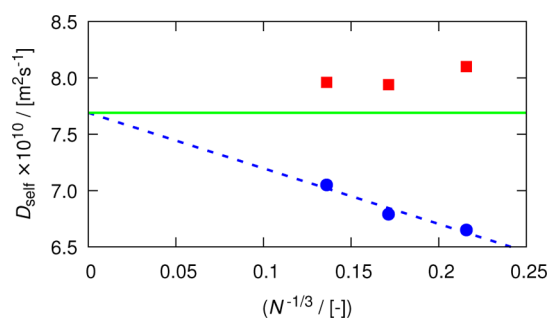
Figure 5. Self-diffusion coefficient of 12-crown-4 at 363 K for different system sizes. Blue circles represent self-diffusion coefficients directly computed from MD results and red squares are the corrected self-diffusion coefficients with the Yeh and Hummer correction (eq 3). The blue dashed line is fitted to the MD simulations and the green line is the extrapolated self-diffusion coefficient in the thermodynamic limit.

increase in the self-diffusion coefficient as the size of the system increases. Although the YH correction slightly overpredicts the finite-size effect, this correction provides a more reliable estimate of the self-diffusion coefficient in the thermodynamic limit. Hence, we report the corrected values for the pure crown-ethers.

The computed viscosities of the crown-ethers at several temperatures are compared with the experiments in Figure 6. It
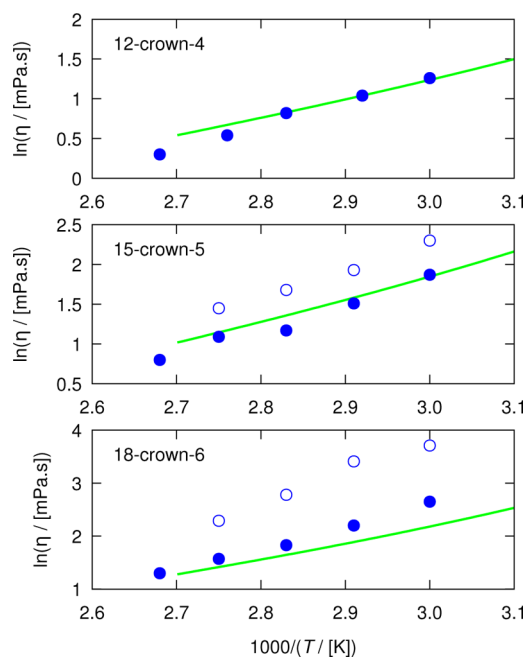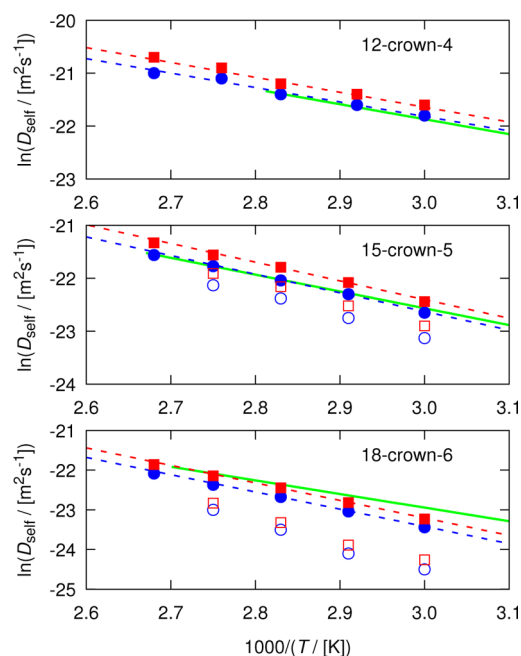

Figure 6. Viscosity of the 12-crown-4, 15-crown-5, and 18-crown-6 as functions of temperature based on the linear ether TraPPE (open symbols) and the refined TraPPE (closed symbols) force fields. Green lines represent experimental data. The simulation results are available in the Supporting Information.

can be seen from the figure that the linear ether TraPPE force field performs poorly. As explained earlier, this force field predicts a solid state for 12-crown-4 at room or elevated temperatures. The agreement between the experiments and the simulation results for 15-crown-5 and 18-crown-6 is also rather weak. However, the results of the refined TraPPE force field correspond closely to the experiments. The maximum

deviations in the viscosity of 12-crown-4 and 15-crown-5 are 10% and 20%. A maximum deviation of 57% in the viscosity of 18-crown-6 is observed at 333 K, and the deviation decreases to 15% as the temperature increases to 363 K. Evidently, the computed viscosity of 18-crown-6 is more sensitive to temperature than the experiments while the simulation results of 12-crown-4 and 15-crown-5 show a similar sensitivity to temperature as the experiments.

It is interesting to compare the viscosity of the crown-ethers with their linear counterparts, namely polyethylene glycol dimethyl ethers (PEGDME). PEGDMEs consist of ether groups like crown-ethers, except that they are linear molecules without any ring in their structure. PEGDMEs are used in industry as solvents for carbon capture and acid gas removal processes under the trade name of Selexol.[59] The viscosity of PEGDME is 3.18 mPa·s at 333 K.[60] At the same temperature, the viscosities of 12-crown-4, 15-crown-5, and 18-crown-6 are 3.47, 6.40, and 8.94 mPa·s, respectively.[61] At the same conditions, PEGDME has a comparable viscosity with 12-crown-4 and a lower viscosity than the other crown-ethers.

The computed self-diffusion coefficients with and without the YH correction are shown together in Figure 7 to emphasize

Figure 7. Self-diffusion of the 12-crown-4, 15-crown-5, and 18-crown-6 at different temperatures, computed from the linear ether TraPPE (open symbols) and the refined TraPPE (closed symbols) force fields. Experimental data are shown with green lines. The linear ether TraPPE force field predicts a solid system for 12-crown-4 for the shown temperatures. The self-diffusion coefficients without and with the inclusion of the YH correction are shown with blue circles/dashed lines and the red squares/dashed lines, respectively. The simulation results are available in the Supporting Information.

the importance of including the YH correction. For our simulations consisting of 80−100 crown-ether molecules, the YH correction can be as large as 20% of the value in the thermodynamic limit. Similar to the viscosity and density, the refined TraPPE force field performs more accurately than the linear ether TraPPE force field. The computed self-diffusion coefficients are fitted to the Arrhenius equation:[62]

$$\ln(D/(\mathrm{m}^2 \cdot \mathrm{s}^{-1})) = \ln D_0 - \frac{E_a}{RT} \qquad (4)$$

where D_0, E_a, R are the pre-exponential factor, the activation energy, and the universal gas constant. D_0 and E_a are computed for the crown-ethers and are listed in Table 2. The activation

Table 2. Comparison between the Fitted Parameters of the Self-Diffusion Coefficients of the Crown-Ethers to the Arrhenius Equation (Eq 4) from the Simulations and Experiments[61]

	simulations		experiments[61]	
	$E_a/[\mathrm{kJ/mol}]$	$\ln(D_0/[\mathrm{m}^2/\mathrm{s}])$	$E_a/[\mathrm{kJ/mol}]$	$\ln(D_0/[\mathrm{m}^2/\mathrm{s}])$
12-crown-4	23.4	−13.2	23.5	−13.4
15-crown-5	29.4	−11.8	26.4	−13.0
18-crown-6	36.7	−10.0	28.5	−12.7

energies of the simulation results are similar to the experimental data except for 18-crown-6. Similar to the viscosity, the self-diffusion coefficient of 18-crown-6 is more sensitive to temperature than the experiments, and the maximum deviation occurs at 333 K. This underprediction of the self-diffusion coefficient and overprediction of the viscosity (Figures 6 and 7) are consistent with the quasi-universal correlations that Rosenfeld proposed in his works.[63,64] Rosenfeld in his article states that the transport properties of a system such as the diffusion coefficient, thermal conductivity, and viscosity are interconnected by means of the reduced excess entropy.

The refined TraPPE force field developed in this study shows high accuracy in predicting the density and transport properties of pure crown-ethers. As this force field is based on the TraPPE force field and the only alteration is the parameters of the torsional potentials, it can be deduced that torsional potentials are important to correctly reproduce the structure and dynamics of the crown-ether molecules in the liquid phase.

Solubility of Natural Gas Components. MC simulations in the osmotic ensemble are employed to study the solubility of the main natural gas components, that are CH_4, CO_2, and N_2, in the crown-ethers. 100 molecules of 12-crown-4 or 80 molecules of 15-crown-5 are inserted initially in the simulation box, which is held in contact with the gas reservoir. As explained earlier, the crown-ethers are considered nonvolatile, and the number of crown-ether molecules remains constant. MC simulations were carried out for these three gases in 12-crown-4 and 15-crown-5 at three pressures and four temperatures. All solubility results are provided in the Supporting Information. As an example, Figure 8 shows the absorption isotherms of the three gases at 333 K. It can be seen that CO_2 has the highest solubility for both 12-crown-4 and 15-crown-5 followed by CH_4 and N_2. Due to the large solubility difference, the separation of CO_2 from CH_4 and N_2 using crown-ethers is feasible.

The resultant solubility data are used to compute the Henry coefficients of the gases in the crown-ethers. The Henry coefficient for the absorption of a gas in a dilute mixture is defined as[62]

$$H_{12} = \lim_{x \to 0} \frac{f_{\mathrm{gas}}}{x} \qquad (5)$$

where f_{gas} and x are the fugacity of the gas and the molefraction of the solute in the mixture, respectively. The computed Henry coefficients at different temperatures are provided in the
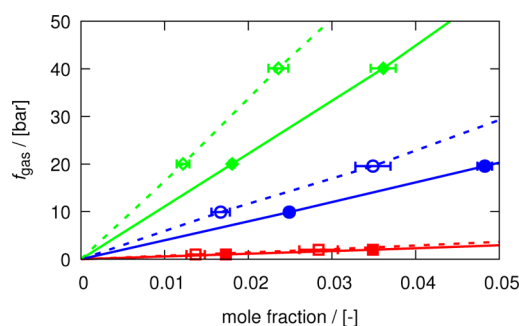
Figure 8. Solubility of CO_2 (red squares/lines), CH_4 (blue circles/lines), and N_2 (green diamonds/lines) in 12-crown-4 (closed symbols/solid lines) and 15-crown-5 (open symbols/dashed lines) at 333 K. The results are fitted to eq 4, whose parameters are provided in Table 2. The simulation results are available in the Supporting Information.

Supporting Information. In Table 3, the Henry coefficients of the solutes in 12-crown-4 (at 303 K) and 15-crown-5 (at 308

Table 3. Computed Henry Coefficients of CO_2, CH_4, and N_2 in 12-Crown-4 and 15-Crown-5[a]

	CO_2	CH_4	N_2
12-crown-4 (303 K)	35.9 (33.6[67])	390	1250 (1430[67])
15-crown-5 (308 K)	45.9 (42.0[67])	550	1620 (1240[67])
PEGDME (313 K)	(43,[68] 47,[69] 56.1[70])	(387[71])	(1680[70])

[a]Data in parentheses are the available experimental data. All values are in bar.

K) are reported and compared with the available experimental data as well as the Henry coefficients of PEGDME (at 313 K). The agreement between the experiments and simulation results suggests that the rigid structure of the crown-ethers may have small influence on the solubility results. The densities of rigid 12-crown-4 and 15-crown-5 are computed using MC simulations and reported in the Supporting Information. The computed densities from MC simulations are always under-predicted, which may have some effects on the gas solubility since molar volumes are important for gas solubilities. However, the effect of rigid molecules on gas solubility cannot quantitatively be examined unless the solubility results in both rigid and flexible molecules of the crown-ethers are compared. Moreover, the Henry coefficients of the gases in the crown-ethers are compared to those of the linear PEGDMEs in Table 3. Both the linear and cyclic molecules have similar Henry coefficients, so a similar CO_2 removal performance as PEGDMEs is expected from the crown-ethers.

The ideal selectivity of two gases, for instance CO_2 and CH_4, in a solvent can be defined as the ratio of their Henry coefficients:[62]

$$S_{CO_2/CH_4} = \frac{H_{CH_4}}{H_{CO_2}} \qquad (6)$$

The ideal CO_2/CH_4 selectivity in 12-crown-4 (303 K), 15-crown-5 (308 K), and PEGDME (313 K) are, respectively, 11.0, 13.2, and 8.2 based on the data of Table 3. The comparable CO_2/CH_4 selectivity of crown-ethers to PEGDMEs (Selexol) along with their low viscosity show the potential of crown-ethers for CO_2 separation from natural gas.

The Gibbs free energy ($\Delta_{abs}G$), enthalpy ($\Delta_{abs}H$), and entropy ($\Delta_{abs}S$) of absorption can be calculated from the Henry coefficients of the gases as functions of temperature:[62]

$$\Delta_{abs}G = RT[\ln(H_{12}/\text{bar})] \quad (7)$$

$$\Delta_{abs}H = -RT^2 \left[\frac{\partial \ln(H_{12}/\text{bar})}{\partial T} \right] \quad (8)$$

$$\Delta_{abs}S = -RT \left[\frac{\partial \ln(H_{12}/\text{bar})}{\partial T} \right] - R\ln(H_{12}/\text{bar}) \quad (9)$$

These equations can be solved provided that a functional form for H_{12} is available as a function of temperature. We use a simple two-parameter equation to specify the temperature dependency of Henry coefficients:[62]

$$\ln(H_{12}/[\text{bar}]) = a_0 + \frac{a_1}{T} \quad (10)$$

Figure 9 shows the computed Henry coefficients and the fitted lines to eq 10. The Henry coefficients of low soluble gases
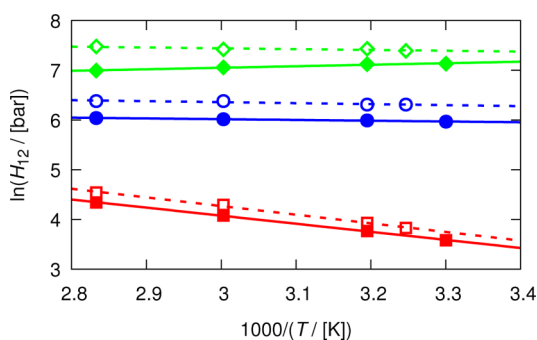

Figure 9. Henry coefficients of CO_2 (red squares/lines), CH_4 (blue circles/lines), and N_2 (green diamonds/lines) in 12-crown-4 (closed symbols/solid lines) and 15-crown-5 (open symbols/dashed lines) at different temperatures. The lines are fitted to eq 10 and the fitted parameters are listed in Table 4.

(CH_4 and N_2) do not strongly depend on the temperature. This weak correlation results in a gradual slope of the lines for CH_4 and N_2, leading to low enthalpies of absorption, as reported in Table 4. The observed solubility trend ($CO_2 > CH_4 > H_2$) is consistent with the enthalpy of absorption of the gases in 12-crown-4 and 15-crown-5. For all the gases, the MC simulations predict a higher solubility in 12-crown-4 than in 15-crown-5. This is remarkable since the solubility of gases generally increases with increasing molecular weight of solvents. Since the enthalpy of absorption of the gases in 12-crown-4 and

15-crown-5 are similar, the difference in the solubilities can be caused by an entropic effect, which is consistent with the $\Delta_{abs}S$ values reported in Table 4. Therefore, it seems that the boat-like shape of 12-crown-4 (shown in the Supporting Information) may be more favorable to accommodate gas molecules compared to the more flat-shaped 15-crown-5 molecules.

In general, the low diffusion of a solute in a solvent as well as the high viscosity of that mixture are the limiting factors in separation processes. As CO_2 has the highest solubility among the studied gases in the crown-ethers, a high diffusion coefficient and low viscosity of the mixture of CO_2 and crown-ethers are appealing for a CO_2 removal process. Here, the transport properties of mixtures of 9%-mole CO_2 in the crown-ethers at different temperatures ranging from 333 to 363 K are studied. According to the computed Henry coefficients, this molefraction approximately corresponds to the partial pressures of CO_2 ranging from 3 to 10 bar in the gas phase. To set up the simulation systems, 10, 8, and 8 CO_2 molecules are respectively added to 100, 80, and 80 molecules of 12-crown-4, 15-crown-5, and 18-crown-6 in the simulation box.

Figure 10 illustrates the self-diffusion coefficient of CO_2 and viscosity of the CO_2-crown-ether mixtures. The results are
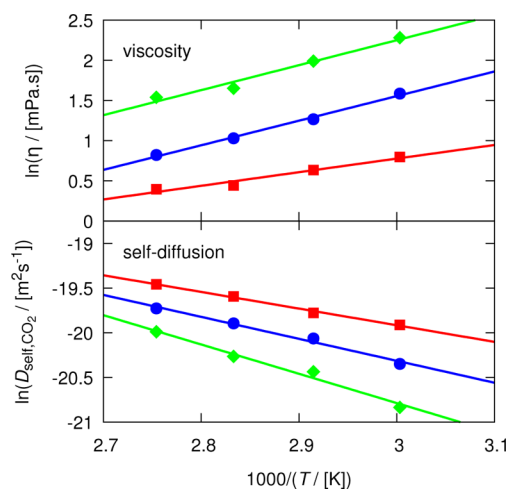
Figure 10. Viscosity and self-diffusion coefficient of CO_2 in the mixtures of 9%-mole CO_2 and 12-crown-4 (red squares/line), 15-crown-5 (blue circles/line), and 18-crown-6 (green diamonds/line) at different temperatures. The lines are fitted to eq 4 and the parameters are available in Table 5. The simulation results are available in the Supporting Information.

provided in the Supporting Information. These data were fitted to the Arrhenius eq (eq 4) so that the transport properties at

Table 4. Thermodynamic Parameters Fitted To the Henry Coefficients of CO_2, CH_4, and N_2 in 12-Crown-4 and 15-Crown-5 Using Eq 10[a]

		a_0 [-]	a_1 [K]	$\Delta_{abs}G$ [kJ/mol]	$\Delta_{abs}H$ [kJ/mol]	$\Delta_{abs}S$ [J/mol·K]
12-crown-4	CO_2	8.94	−1623	9.0	−13.5	−74.4
	CH_4	6.47	−153	15.0	−1.3	−53.8
	N_2	6.14	305	18.0	2.5	−51.0
15-crown-5	CO_2	9.48	−1736	9.4	−14.4	−78.8
	CH_4	6.68	−198	15.9	−1.6	−57.8
	N_2	7.93	−164	18.6	−1.4	−66.0

[a]The Gibbs free energy ($\Delta_{abs}G$), enthalpy ($\Delta_{abs}H$), and entropy ($\Delta_{abs}S$) of absorptions are calculated from eq 7 to 9 at a temperature of 303 K and a pressure of 1 bar.

other temperatures can be calculated. The fitted parameters are listed in Table 5. A comparison between Figures 10 and 6

Table 5. Parameters Fitted To Eq 4 for the Self-Diffusion Coefficient of CO_2 and Viscosity of the Mixtures of 9%-Mole CO_2 and the Crown-Ethers

	viscosity		self-diffusion	
	$E_a/$ [kJ/mol]	$\ln(\eta_0/[\text{mPa·s}])$	$E_a/$ [kJ/mol]	$\ln(D_0/[\text{m}^2/\text{s}])$
12-crown-4	14.1	−4.3	15.5	−14.3
15-crown-5	25.4	−7.6	20.4	−12.9
18-crown-6	25.8	−7.1	27.3	−11.0

shows that the addition of CO_2 to the crown-ethers decreases the viscosity of the mixture about 30%. The self-diffusion coefficient of CO_2 is also one order of magnitude larger than the self-diffusion of the pure crown-ethers. As the self-diffusion of CO_2 is very large, the YH correction (eq 3) for this system is comparatively small and within the uncertainty of the results. Therefore, we do not include any finite-size correction. This is in agreement with the results of Moultos et al.[65,66] who concluded that there is no specific finite-size effect on the self-diffusion of a solute in a mixture.

CONCLUSIONS

Crown-ethers, or cyclic molecules consisting of ether groups, have recently been proposed for gas separation processes as a proper solvent for porous liquids. This research investigated the thermodynamic and transport properties of several crown-ethers, which are 12-crown-4, 15-crown-5, and 18-crown-6, using force field-based molecular simulations. Since the TraPPE force field developed for linear molecules cannot be employed for cyclic molecules, a new set of torsional potential parameters were computed for crown-ethers from DFT calculations. The transferability of the developed force field should be comparable to the TraPPE force field, which means that the developed force field can be combined with other types of crown-ethers as well as other biomolecules defined by the TraPPE force field. MD simulations were carried out to compute the density, viscosity, and self-diffusion coefficient of the pure crown-ethers. Monte Carlo simulations were used to study the solubility of natural gas components, that are CH_4, N_2, and CO_2, in the crown-ethers. The computed thermodynamic and transport properties correspond closely to the experiments, suggesting the accuracy of the new force field, which is also transferable to other cyclic-ether molecules. Furthermore, the comparable transport properties and the CO_2/CH_4 selectivity of the studied crown-ethers, especially 12-crown-4, with polyethylene glycol dimethyl ethers indicate the potential of the crown-ether in gas treatment processes.

ASSOCIATED CONTENT

Ⓢ Supporting Information
The Supporting Information is available free of charge on the ACS Publications website at DOI: 10.1021/acs.jpcb.7b06547.

Thermodynamic/transport results and the employed force field parameters as well as the structure of the crown-ethers from the DFT and the crystalline structure of 12-crown-4 (PDF)

AUTHOR INFORMATION

Corresponding Author
*E-mail: t.j.h.vlugt@tudelft.nl.

ORCID ⃝
Seyed Hossein Jamali: 0000-0002-4198-0901
Wim Buijs: 0000-0003-3273-5063
Thijs J. H. Vlugt: 0000-0003-3059-8712

Notes
The authors declare no competing financial interest.

REFERENCES

(1) Pedersen, C. J. Cyclic Polyethers and their Complexes with Metal Salts. *J. Am. Chem. Soc.* **1967**, *89*, 7017−7036.
(2) Swidan, A.; Macdonald, C. L. B. Polyether Complexes of Groups 13 and 14. *Chem. Soc. Rev.* **2016**, *45*, 3883−3915.
(3) Mohammadzadeh Kakhki, R. Application of Crown Ethers as Stationary Phase in the Chromatographic Methods. *J. Inclusion Phenom. Mol. Recognit. Chem.* **2013**, *75*, 11−22.
(4) Arnaud-Neu, F.; Delgado, R.; Chaves, S. Critical Evaluation of Stability Constants and Thermodynamic Functions of Metal Complexes of Crown Ethers (IUPAC technical report). *Pure Appl. Chem.* **2003**, *75*, 71−102.
(5) Yoshio, M.; Noguchi, H. Crown Ethers for Chemical Analysis: A Review. *Anal. Lett.* **1982**, *15*, 1197−1276.
(6) Gokel, G. W.; Leevy, W. M.; Weber, M. E. Crown Ethers: Sensors for Ions and Molecular Scaffolds for Materials and Biological Models. *Chem. Rev.* **2004**, *104*, 2723−2750.
(7) Giri, N.; del Pópolo, M. G.; Melaugh, G.; Greenaway, R. L.; Rätzke, K.; Koschine, T.; Pison, L.; Gomes, M. F. C.; Cooper, A. I.; James, S. L. Liquids with Permanent Porosity. *Nature* **2015**, *527*, 216−220.
(8) James, S. L. The Dam Bursts for Porous Liquids. *Adv. Mater.* **2016**, *28*, 5712−5716.
(9) Das, S.; Heasman, P.; Ben, T.; Qiu, S. Porous Organic Materials: Strategic Design and Structure-Function Correlation. *Chem. Rev.* **2017**, *117*, 1515−1563.
(10) O'Reilly, N.; Giri, N.; James, S. L. Porous Liquids. *Chem. - Eur. J.* **2007**, *13*, 3020−3025.
(11) Mastalerz, M. Materials Chemistry: Liquefied Molecular Loles. *Nature* **2015**, *527*, 174−176.
(12) Zhang, J.; Chai, S.-H.; Qiao, Z.-A.; Mahurin, S. M.; Chen, J.; Fang, Y.; Wan, S.; Nelson, K.; Zhang, P.; Dai, S. Porous Liquids: A Promising Class of Media for Gas Separation. *Angew. Chem., Int. Ed.* **2015**, *54*, 932−936.
(13) Zhang, F.; Yang, F.; Huang, J.; Sumpter, B. G.; Qiao, R. Thermodynamics and Kinetics of Gas Storage in Porous Liquids. *J. Phys. Chem. B* **2016**, *120*, 7195−7200.
(14) Greenaway, R. L.; Holden, D.; Eden, E. G. B.; Stephenson, A.; Yong, C. W.; Bennison, M. J.; Hasell, T.; Briggs, M. E.; James, S. L.; Cooper, A. I. Understanding Gas Capacity, Guest Selectivity, and Diffusion in Porous Liquids. *Chem. Sci.* **2017**, *8*, 2640−2651.
(15) Cooper, A. I. Porous Molecular Solids and Liquids. *ACS Cent. Sci.* **2017**, *3*, 544−553.
(16) Zhang, F.; He, Y.; Huang, J.; Sumpter, B. G.; Qiao, R. Multicomponent Gas Storage in Organic Cage Molecules. *J. Phys. Chem. C* **2017**, *121*, 12426−12433.

(17) van Eerden, J.; Harkema, S.; Feil, D. Molecular Dynamics of 18-Crown-6 Complexes with Alkali-Metal Cations: Calculation of Relative Free Energies of Complexation. *J. Phys. Chem.* **1988**, *92*, 5076−5079.

(18) Grootenhuis, P. D. J.; Kollman, P. A. Molecular Mechanics and Dynamics Studies of Crown Ether-Cation Interactions: Free Energy Calculations on the Cation Selectivity of Dibenzo-18-Crown-6 and Dibenzo-30-Crown-10. *J. Am. Chem. Soc.* **1989**, *111*, 2152−2158.

(19) Dang, L. X.; Kollman, P. A. Free Energy of Association of the 18-Crown-6:K⁺ Complex in Water: A Molecular Dynamics Simulation. *J. Am. Chem. Soc.* **1990**, *112*, 5716−5720.

(20) Wipff, G. Molecular Modeling Studies on Molecular Recognition: Crown Ethers, Cryptands and Cryptates. From Static Models in vacuo to Dynamical Models in Solution. *J. Coord. Chem.* **1992**, *27*, 7−37.

(21) Guilbaud, P.; Wipff, G. Hydration of Uranyl (UO_2^{2+}) Cation and its Nitrate Ion and 18-Crown-6 Adducts Studied by Molecular Dynamics Simulations. *J. Phys. Chem.* **1993**, *97*, 5685−5692.

(22) Troxler, L.; Wipff, G. Conformation and Dynamics of 18-Crown-6, Cryptand 222, and Their Cation Complexes in Acetonitrile Studied by Molecular Dynamics Simulations. *J. Am. Chem. Soc.* **1994**, *116*, 1468−1480.

(23) Dang, L. X. Mechanism and Thermodynamics of Ion Selectivity in Aqueous Solutions of 18-Crown-6 Ether: A Molecular Dynamics Study. *J. Am. Chem. Soc.* **1995**, *117*, 6954−6960.

(24) Dang, L. X.; Kollman, P. A. Free Energy of Association of the K⁺: 18-Crown-6 Complex in Water: A New molecular Dynamics Study. *J. Phys. Chem.* **1995**, *99*, 55−58.

(25) Zwier, M. C.; Kaus, J. W.; Chong, L. T. Efficient Explicit-Solvent Molecular Dynamics Simulations of Molecular Association Kinetics: Methane/Methane, Na⁺/Cl⁻, Methane/Benzene, and K⁺)/18-Crown-6 Ether. *J. Chem. Theory Comput.* **2011**, *7*, 1189−1197.

(26) Billeter, M.; Howard, A. E.; Kuntz, I. D.; Kollman, P. A. A New Technique to Calculate Low-Energy Conformations of Cyclic Molecules Utilizing the Ellipsoid Algorithm and Molecular Dynamics: Application to 18-Crown-6. *J. Am. Chem. Soc.* **1988**, *110*, 8385−8391.

(27) van Eerden, J.; Harkema, S.; Feil, D. Molecular-Dynamics Simulation of Crystalline 18-Crown-6: Thermal Shortening of Covalent Bonds. *Acta Crystallogr., Sect. B: Struct. Sci.* **1990**, *46*, 222−229.

(28) Weiner, S. J.; Kollman, P. A.; Case, D. A.; Singh, U. C.; Ghio, C.; Alagona, G.; Profeta, S.; Weiner, P. A new force field for molecular mechanical simulation of nucleic acids and proteins. *J. Am. Chem. Soc.* **1984**, *106*, 765−784.

(29) Martin, M. G.; Siepmann, J. I. Transferable Potentials for Phase Equilibria. 1. United-Atom Description of n-alkanes. *J. Phys. Chem. B* **1998**, *102*, 2569−2577.

(30) Potoff, J. J.; Siepmann, J. I. Vapor-Liquid Equilibria of Mixtures Containing Alkanes, Carbon Dioxide, and Nitrogen. *AIChE J.* **2001**, *47*, 1676−1682.

(31) Shah, M. S.; Tsapatsis, M.; Siepmann, J. I. Development of the Transferable Potentials for Phase Equilibria Model for Hydrogen Sulfide. *J. Phys. Chem. B* **2015**, *119*, 7041−7052.

(32) Stubbs, J. M.; Potoff, J. J.; Siepmann, J. I. Transferable Potentials for Phase Equilibria. 6. United-Atom Description for Ethers, Glycols, Ketones, and Aldehydes. *J. Phys. Chem. B* **2004**, *108*, 17596−17605.

(33) Keasler, S. J.; Charan, S. M.; Wick, C. D.; Economou, I. G.; Siepmann, J. I. Transferable Potentials for Phase Equilibria-United Atom Description of Five- and Six-Membered Cyclic Alkanes and Ethers. *J. Phys. Chem. B* **2012**, *116*, 11234−11246.

(34) *Spartan'14*; Wavefunction, Inc.: Irvine, CA, 2014.

(35) *Optimization Toolbox User's Guide*; MathWorks, Inc.: Natick, MA, 2016.

(36) Dubbeldam, D.; Calero, S.; Ellis, D. E.; Snurr, R. Q. RASPA: Molecular Simulation Software for Adsorption and Diffusion in Flexible Nanoporous Materials. *Mol. Simul.* **2016**, *42*, 81−101.

(37) Dubbeldam, D.; Torres-Knoop, A.; Walton, K. S. On the inner workings of Monte Carlo codes. *Mol. Simul.* **2013**, *39*, 1253−1292.

(38) Plimpton, S. Fast Parallel Algorithms for Short-Range Molecular Dynamics. *J. Comput. Phys.* **1995**, *117*, 1−19.

(39) Cygan, R. T.; Romanov, V. N.; Myshakin, E. M. Molecular Simulation of Carbon Dioxide Capture by Montmorillonite Using an Accurate and Flexible Force Field. *J. Phys. Chem. C* **2012**, *116*, 13079−13091.

(40) Allen, M. P.; Tildesley, D. J. *Computer Simulation of Liquids*; Oxford University Press: New York, 1989.

(41) Frenkel, D.; Smit, B. *Understanding Molecular Simulation: From Algorithms to Applications*, 2nd ed.; Academic Press: London, 2002.

(42) Müller-Plathe, F. Reversing the Perturbation in Nonequilibrium Molecular Dynamics: An Easy Way to Calculate the Shear Viscosity of Fluids. *Phys. Rev. E: Stat. Phys., Plasmas, Fluids, Relat. Interdiscip. Top.* **1999**, *59*, 4894−4898.

(43) Arya, G.; Maginn, E. J.; Chang, H.-C. Efficient Viscosity Estimation from Molecular Dynamics Simulation via Momentum Impulse Relaxation. *J. Chem. Phys.* **2000**, *113*, 2079.

(44) Kelkar, M. S.; Rafferty, J. L.; Maginn, E. J.; Siepmann, J. I. Prediction of Viscosities and Vapor-Liquid Equilibria for Five Polyhydric Alcohols by Molecular Simulation. *Fluid Phase Equilib.* **2007**, *260*, 218−231.

(45) Tenney, C. M.; Maginn, E. J. Limitations and Recommendations for the Calculation of Shear Viscosity Using Reverse Nonequilibrium Molecular Dynamics. *J. Chem. Phys.* **2010**, *132*, 014103.

(46) Zhang, Y.; Otani, A.; Maginn, E. J. Reliable Viscosity Calculation from Equilibrium Molecular Dynamics Simulations: A Time Decomposition Method. *J. Chem. Theory Comput.* **2015**, *11*, 3537−3546.

(47) Liu, X.; Schnell, S. K.; Simon, J.-M.; Krüger, P.; Bedeaux, D.; Kjelstrup, S.; Bardow, A.; Vlugt, T. J. H. Diffusion Coefficients from Molecular Dynamics Simulations in Binary and Ternary Mixtures. *Int. J. Thermophys.* **2013**, *34*, 1169−1196.

(48) Shi, W.; Sorescu, D. C.; Luebke, D. R.; Keller, M. J.; Wickramanayake, S. Molecular Simulations and Experimental Studies of Solubility and Diffusivity for Pure and Mixed Gases of H_2, CO_2, and Ar Absorbed in the Ionic Liquid 1- n-Hexyl-3-methylimidazolium Bis(Trifluoromethylsulfonyl)amide ([hmim][Tf₂N]). *J. Phys. Chem. B* **2010**, *114*, 6531−6541.

(49) Liu, H.; Maginn, E. A Molecular Dynamics Investigation of the Structural and Dynamic Properties of the Ionic Liquid 1-n-Butyl-3-methylimidazolium Bis(Trifluoromethanesulfonyl)imide. *J. Chem. Phys.* **2011**, *135*, 124507.

(50) Dubbeldam, D.; Ford, D. C.; Ellis, D. E.; Snurr, R. Q. A New Perspective on the Order-n Algorithm for Computing Correlation Functions. *Mol. Simul.* **2009**, *35*, 1084−1097.

(51) Shi, W.; Maginn, E. J. Continuous Fractional Component Monte Carlo: An Adaptive Biasing Method for Open System Atomistic Simulations. *J. Chem. Theory Comput.* **2007**, *3*, 1451−1463.

(52) Shi, W.; Maginn, E. J. Molecular Simulation and Regular Solution Theory Modeling of Pure and Mixed Gas Absorption in the Ionic Liquid 1-n-Hexyl-3-methylimidazolium Bis-(Trifluoromethylsulfonyl)amide ([hmim][Tf₂N]). *J. Phys. Chem. B* **2008**, *112*, 16710−16720.

(53) Ramdin, M.; Balaji, S. P.; Vicent-Luna, J. M.; Gutiérrez-Sevillano, J. J.; Calero, S.; de Loos, T. W.; Vlugt, T. J. H. Solubility of the Precombustion Gases CO_2, CH_4, CO, H_2, N_2, and H_2S in the Ionic Liquid [bmim][Tf₂N] from Monte Carlo Simulations. *J. Phys. Chem. C* **2014**, *118*, 23599−23604.

(54) Ramdin, M.; Chen, Q.; Balaji, S. P.; Vicent-Luna, J. M.; Torres-Knoop, A.; Dubbeldam, D.; Calero, S.; de Loos, T. W.; Vlugt, T. J. H. Solubilities of CO_2, CH_4, C_2H_6, and SO_2 in Ionic Liquids and Selexol from Monte Carlo Simulations. *J. Comput. Sci.* **2016**, *15*, 74−80.

(55) Ramdin, M.; Balaji, S. P.; Vicent-Luna, J. M.; Torres-Knoop, A.; Chen, Q.; Dubbeldam, D.; Calero, S.; de Loos, T. W.; Vlugt, T. J. H. Computing Bubble-Points of CO_2/CH_4 Gas Mixtures in Ionic Liquids from Monte Carlo Simulations. *Fluid Phase Equilib.* **2016**, *418*, 100−107.

(56) Jamali, S. H.; Ramdin, M.; Becker, T. M.; Torres-Knoop, A.; Dubbeldam, D.; Buijs, W.; Vlugt, T. J. H. Solubility of Sulfur Compounds in Commercial Physical Solvents and an Ionic Liquid from Monte Carlo Simulations. *Fluid Phase Equilib.* **2017**, *433*, 50−55.

(57) Yeh, I.-C.; Hummer, G. System-Size Dependence of Diffusion Coefficients and Viscosities from Molecular Dynamics Simulations with Periodic Boundary Conditions. *J. Phys. Chem. B* **2004**, *108*, 15873−15879.

(58) Moultos, O. A.; Zhang, Y.; Tsimpanogiannis, I. N.; Economou, I. G.; Maginn, E. J. System-Size Corrections for Self-Diffusion Coefficients Calculated from Molecular Dynamics Simulations: The Case of CO_2, n-alkanes, and Poly(Ethylene Glycol) Dimethyl Ethers. *J. Chem. Phys.* **2016**, *145*, 074109.

(59) Kohl, A. L.; Nielsen, R. *Gas Purification*, 5th ed.; Gulf Professional Publishing: Houston, 1997.

(60) Li, J.; Mundhwa, M.; Henni, A. Volumetric Properties, Viscosities, Refractive Indices, and Surface Tensions for Aqueous Genosorb 1753 Solutions. *J. Chem. Eng. Data* **2007**, *52*, 955−958.

(61) Vogel, H.; Weiss, A. Transport Properties of Liquids I. Self-Diffusion, Viscosity and Density of Nearly Spherical and Disk Like Molecules in the Pure Liquid Phase. *Berichte der Bunsengesellschaft füs. Chemie* **1981**, *85*, 539−548.

(62) Prausnitz, J. M.; Lichtenthaler, R. N.; de Azevedo, E. G. *Molecular Thermodynamics of Fluid-Phase Equilibria*; Prentice Hall: NJ, 1998.

(63) Rosenfeld, Y. Relation between the Transport Coefficients and the Internal Entropy of Simple Systems. *Phys. Rev. A: At., Mol., Opt. Phys.* **1977**, *15*, 2545−2549.

(64) Rosenfeld, Y. A Quasi-Universal Scaling Law for Atomic Transport in Simple Fluids. *J. Phys.: Condens. Matter* **1999**, *11*, 5415−5427.

(65) Moultos, O. A.; Orozco, G. A.; Tsimpanogiannis, I. N.; Panagiotopoulos, A. Z.; Economou, I. G. Atomistic Molecular Dynamics Simulations of H_2O Diffusivity in Liquid and Supercritical CO_2. *Mol. Phys.* **2015**, *113*, 2805−2814.

(66) Moultos, O. A.; Tsimpanogiannis, I. N.; Panagiotopoulos, A. Z.; Trusler, J. P. M.; Economou, I. G. Atomistic Molecular Dynamics Simulations of Carbon Dioxide Diffusivity in n-Hexane, n-Decane, n-Hexadecane, Cyclohexane, and Squalane. *J. Phys. Chem. B* **2016**, *120*, 12890−12900.

(67) Linford, R.; Thornhill, D. Solubilities of a Gas in a Crown Ether. *J. Chem. Thermodyn.* **1985**, *17*, 701−702.

(68) Henni, A.; Tontiwachwuthikul, P.; Chakma, A. Solubilities of Carbon Dioxide in Polyethylene Glycol Ethers. *Can. J. Chem. Eng.* **2005**, *83*, 358−361.

(69) Rayer, A. V.; Henni, A.; Tontiwachwuthikul, P. High Pressure Physical Solubility of Carbon Dioxide (CO_2) in Mixed Polyethylene Glycol Dimethyl Ethers (Genosorb 1753). *Can. J. Chem. Eng.* **2012**, *90*, 576−583.

(70) Gainar, I.; Anitescu, G. The Solubility of CO_2, N_2 and H_2 in a Mixture of Dimethylether Polyethylene Glycols at High Pressures. *Fluid Phase Equilib.* **1995**, *109*, 281−289.

(71) Henni, A.; Tontiwachwuthikul, P.; Chakma, A. Solubility Study of Methane and Ethane in Promising Physical Solvents for Natural Gas Sweetening Operations. *J. Chem. Eng. Data* **2006**, *51*, 64−67.